

# Chip scale atomic magnetometers

J. Moreland,<sup>1</sup> J. Kitching,<sup>2</sup> P. D. D. Schwindt,<sup>2</sup> S. Knappe,<sup>2,3</sup> L. Liew,<sup>1</sup> V. Shah,<sup>2,3</sup>  
V. Gerginov,<sup>2,4</sup> Y.-J. Wang,<sup>2,3</sup> and L. Hollberg<sup>2</sup>

<sup>1</sup>Electromagnetics Division and <sup>2</sup>Time and Frequency Division  
National Institute of Standards and Technology  
Boulder, Colorado 80305

<sup>3</sup>Physics Department  
University of Colorado  
Boulder, Colorado 80309

<sup>4</sup>Physics Department  
University of Notre Dame  
Notre Dame, Indiana 46556

## ABSTRACT

We are developing a new class of sensors based on atoms confined in micro-fabricated enclosures. Recent work at the National Institute of Standards and Technology (NIST) has lead to a prototype chip scale atomic clock (CSAC) with remarkable operating characteristics in terms of frequency stability, size, and power consumption. The CSAC fabrication methodology has promise for scaling to wafer level production so that the cost benefits of mass production may be realized. We intend to extend this core CSAC technology to other atomic vapor based micro-systems that will be useful for a variety of measurement applications critical to national security. For example, the precise frequency measurement capabilities afforded by atomic vapor frequency references should allow us to measure small static magnetic fields below 1 pT. We will discuss the principles of a micro-fabricated "hyperfine" magnetometer physics package based on magnetically sensitive hyperfine transitions in an alkali atom recently demonstrated at NIST. This magnetometer has a sensitivity of 50 pT Hz<sup>-1/2</sup> at 10 Hz, a physics-package volume of 12 mm<sup>3</sup> (with a vapor cell volume of 1 mm<sup>3</sup>), and a power dissipation of 200 mW; and there are prospects for significant improvements. In addition we discuss the principles of other approaches based on micro-fabricated atomic vapor cells currently being considered for sub-picotesla measurements based on magneto-optical effects or the direct coupling of the magnetic moment of the atoms to micromechanical oscillators.

## 1. Introduction

Performance requirements for field deployable magnetometers include not only minimum field sensitivity capability but size, power consumption, durability/stability, and cost as well. Microsystems technology development for magnetic sensors that may potentially score well in all of these categories is an active area of research with notable progress on NMR,<sup>1</sup> Hall effect,<sup>2</sup> giant magnetoresistive (GMR),<sup>3</sup> and flux-gate probes.<sup>4</sup> Until recently it was generally believed that sensors based on magnetically sensitive atomic transitions would suffer upon size reduction due to line broadening effects caused by wall collisions in small atomic vapor cells. The question is, Can the components of an atomic magnetometer be fabricated and integrated into a field-deployable chip-scale micro system with superior performance characteristics? Many different types of atomic magnetometers have been developed over the years, with recent focus on atomic optical magnetometers based on spectroscopy or polarimetry with  $1 \text{ fT Hz}^{-1/2}$  sensitivity, rivaling SQUID performance.<sup>5-7</sup> We discuss one approach here in detail based on a micro-fabricated chip scale atomic clock recently demonstrated at NIST. Atomic optical magnetometers have the advantages of being non-cryogenic and not requiring bulky microwave resonators for excitation of atomic transitions, and are thus candidates as the basis for micro-systems development of small, low power, rugged low field sensors. Further, atomic magnetometers are fundamentally accurate given a detailed knowledge of the gyromagnetic ratio  $\gamma$  of the atom. The purpose of this paper is to provide an overview for chip-scale atomic magnetometers underscoring the primary physics and engineering challenges facing micro systems development.

## 2. Summary of chip scale atomic clock development to date

We have recently demonstrated component-level functionality of the three subsystems that comprise a complete chip-scale atomic clock (CSAC): the physics package, the local oscillator and the control electronics.<sup>8-11</sup> The volume of the clock is  $3.5 \text{ cm}^3$ ,  $1/100$  that of the smallest commercial clocks available today; the short-term frequency instability is below  $6 \times 10^{-10}/\sqrt{\text{t}}$ ,  $0 < \text{t} < 100 \text{ s}$ , about 100 times better than current oven-controlled crystal oscillator (OCXO) technology; and the total power consumption is 155 mW at 25 °C, about  $1/100$  that of the smallest commercial clock technology. Many physics and fabrication problems have already been addressed and we see a clear path towards a CSAC volume of 1  $\text{cm}^3$  with frequency stability of  $10^{-11}/\sqrt{\text{t}}$  and power consumption of 30 mW with the potential for commercialization in a few years. Clearly the micro-systems approach using micro-fabrication methods developed for micro-electromechanical systems (MEMS) has paid off. The device's design is amenable to wafer-level fabrication and assembly in which wafers containing hundreds of each component could be stacked to allow multiple sensors to be assembled simultaneously, potentially reducing the manufacturing costs dramatically. In principle, we feel this technology can be applied to a broader range of applications that would benefit from a marriage of atomic physics and MEMS that includes not only magnetometers but gyroscopes and high resolution saturation laser spectroscopy as well.

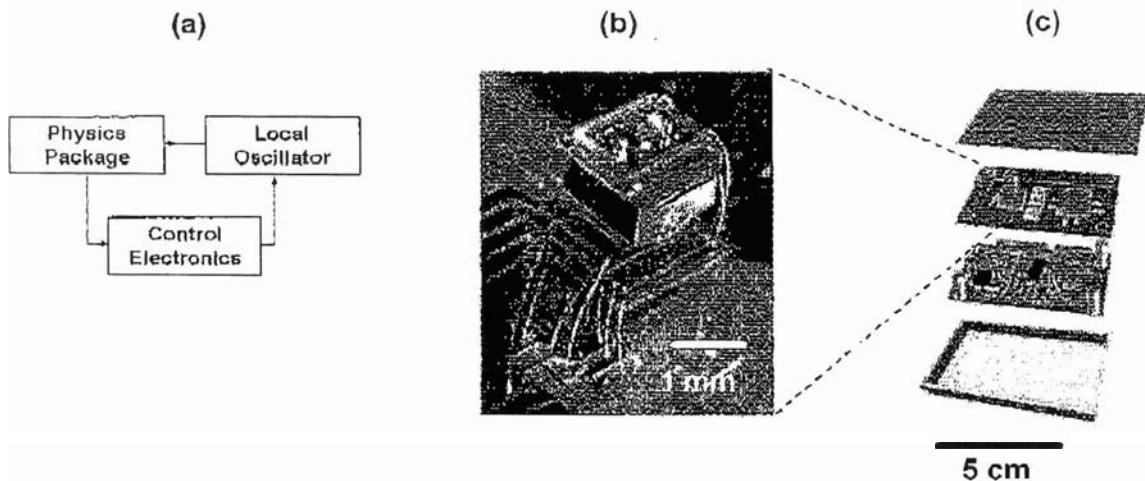


**Figure 1.** (a) A CSAC consists of three major components: the physics package, a local oscillator, and the feedback control electronics for frequency stabilization and temperature control of various sub-components. (b) The physics package is a stack of micro-fabricated components integrating thermistors, thermal isolation components, optics, a heated vapor cell, and a photo detector. (c) The major components will be assembled into an evacuated shielded enclosure with a lower printed circuit board having the control electronics and the upper board having the local oscillator and the physics package.

### 3. A chip scale magnetometer based on atomic hyperfine transitions

We have adopted the CSAC technology described above to perform atom-optical magnetometry based on coherent population trapping (CPT) spectroscopy.<sup>12</sup> In the CPT scheme microwaves need not be applied directly to the atoms. Instead, an optical field is modulated at the atomic hyperfine frequency, resulting in two optical fields (laser side bands), separated by the atomic oscillation frequency.<sup>13</sup> This eliminates the need for microwave resonant cavities that can be problematic when it comes to miniaturization of magnetometer components. Due to the CPT effect, the absorption of these two optical fields is altered when the separation frequency of the laser side bands exactly equals the atomic hyperfine splitting and the atoms are populated into a narrow “dark state.” The transmission peak can be used to lock the local oscillator frequency to the atomic transition.

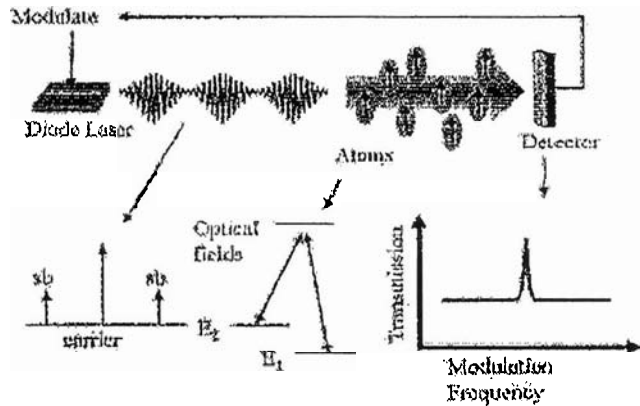


**Figure 2.** CPT excitation of atomic hyperfine transitions by means of a modulated lasersidebands (sb).

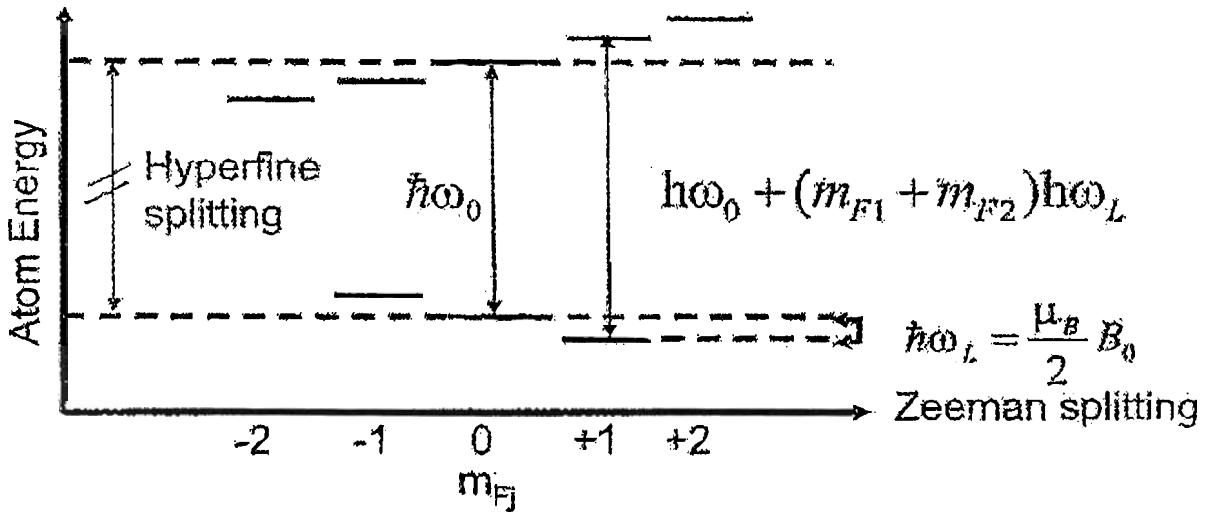


**Figure 3. Magnetic shifts of the atomic states showing hyperfine and Zeeman splitting and the magnetically sensitive transitions.**

The hyperfine states are split by the application of a magnetic field as shown in Fig. 3. By performing feedback on the CPT transition between the magnetically insensitive hyperfine states of the atoms the device is useful as a clock but not as a magnetometer. The magnetic field can be measured, however, by probing the hyperfine transitions between two magnetically sensitive Zeeman states at optical frequencies<sup>14,15</sup> or by probing the Zeeman splitting directly at low frequencies (see discussion below). To measure the magnetic flux density experienced by the <sup>87</sup>Rb atoms optically, we probe the 5S<sub>1/2</sub> ground state hyperfine splitting between two magnetically sensitive Zeeman states via a CPT resonance. The energy difference between two Zeeman states in the  $F=1$  and  $F=2$  hyperfine manifolds at small magnetic fields is given approximately by

$$\hbar\omega_{m_1, m_2} \approx \hbar\omega_{0,0} + (m_1 + m_2)\gamma B, \quad (1)$$

where  $\hbar\omega_{0,0}$  is the energy difference between the magnetically insensitive states  $|F=1, m_1=0\rangle$  and  $|F=2, m_2=0\rangle$ ,  $m_1$  and  $m_2$  are respectively the azimuthal quantum numbers for the  $F=1$  and  $F=2$  states,  $\gamma$  is the gyromagnetic ratio of the atom, and  $B$  is the magnitude of the magnetic flux density. Thus, the CPT magnetometer is a scalar detector, but it can be operated as a vector magnetometer, sensitive to a single field component, by applying a bias field along the direction of measurement.

An assembled chip scale atomic magnetometer physics package is shown in Fig. 4. The core of the sensor is a micro fabricated rubidium vapor cell that is made by anodically bonding a glass wafer to either side of a 1 mm-thick silicon wafer with a 1 mm<sup>2</sup> hole etched through it. The cell is filled with <sup>87</sup>Rb and a buffer gas containing a mixture of argon at 11 kPa and neon at 21 kPa that reduces the frequency decohering Rb-cell-wall collisions. To create sufficient atomic density in the small cell, we heat it to 120 °C by dissipating 160 mW with two transparent indium-tin-oxide (ITO) heaters placed on either side of the cell. The cell is illuminated with a vertical-cavity surface-emitting laser (VCSEL). The light from the

VCSEL passes through a micro-optics package that attenuates the power to 5  $\mu\text{W}$ , circularly polarizes the beam, and collimates it to a diameter of 170  $\mu\text{m}$ . After the beam passes through the cell, it is detected by a PIN silicon photodiode. When all components are stacked together, the sensor is 3.9 mm high and occupies a volume of 12  $\text{mm}^3$ .

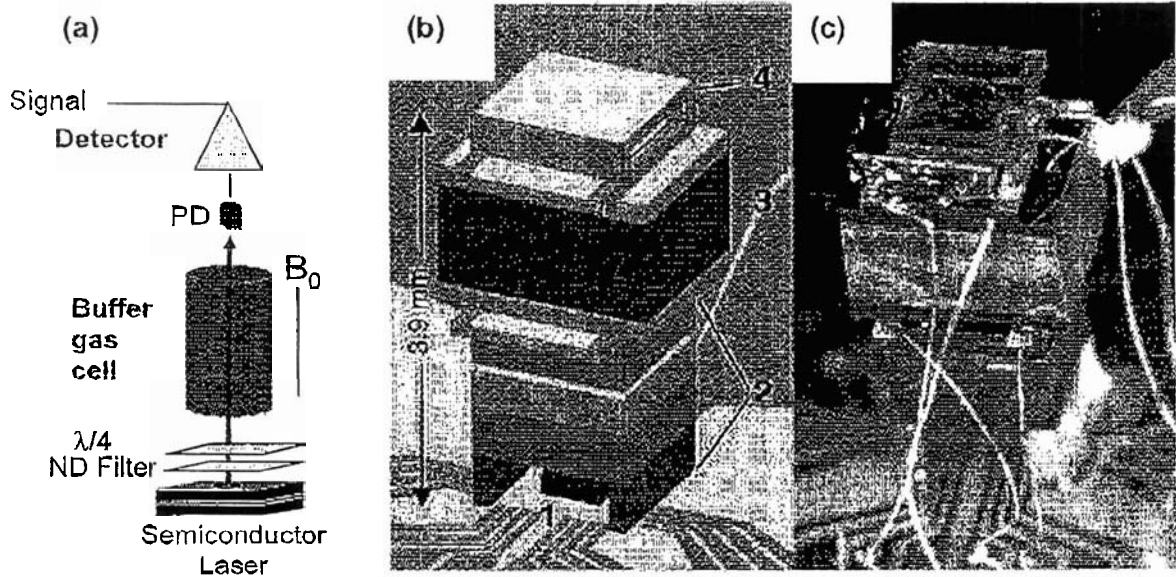


**Figure 4.** (a) CPT atomic magnetometer. (b) The micro-fabricated components of a chip-scale CPT magnetometer physics package are: 1 - VCSEL, 2-optics package including (from bottom to top) a glass spacer, a neutral-density filter, 2 - a refractive micro-lens surrounded by an epoxy spacer, a quartz  $1/4$  wave plate, and a neutral-density filter, 3 -  $^{87}\text{Rb}$  vapor cell with transparent ITO heaters above and below it, and 4 - photodiode assembly. (c) Photograph of the magnetic sensor. Gold wire bonds provide the electrical connections from the base plate to the ITO heaters and the photodiode (figure from ref. 12).

To excite the CPT resonance, we tune the VCSEL to the D1 line of  $^{87}\text{Rb}$  at 795 nm. A local oscillator modulates the current to the VCSEL at 3.4 GHz, half the hyperfine splitting of the Rb ground state, creating two first-order sidebands that are simultaneously resonant with the two hyperfine ground states to the  $P_{1/2}$  excited state (Fig. 5(b)).<sup>16</sup> When the frequency difference between the first-order sidebands is equal to the splitting between two Zeeman states, the atoms are optically pumped into a coherent dark state. We then observe a reduction of the absorbed light power, for example, by 5.4 % when the current modulation frequency is tuned to the  $|1,-1\rangle - |2,-1\rangle$  resonance.

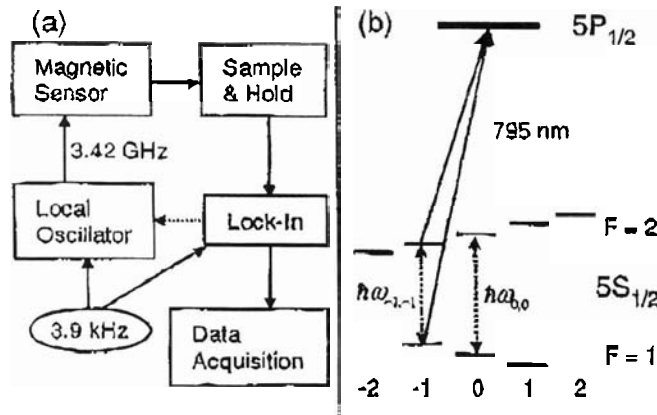


**Figure 5.** (a) The experimental setup for detecting the magnetic flux density. The dashed arrow indicates that the lock-in amplifier can provide feedback to the local oscillator, allowing the local oscillator to track large changes in magnetic field. The magnetometer is run open loop for the data in Figs. 6a and 6b. (b) Energy level diagram (not to scale) of  $^{87}\text{Rb}$  showing the resonant first-order sidebands of the VCSEL (figure from ref. 12).

When the magnetometer is in operation, the frequency of the local oscillator is tuned to approximately  $\omega_{-1,-1}$  (Fig. 5(b)). The magnetometer achieves maximal sensitivity in a magnetic field that is either parallel or transverse to the light propagation direction. For convenience we operate with a parallel field, and thus selection rules allow CPT resonances to form only when  $m_1 - m_2 = 0$ .<sup>17</sup> We frequency modulate the local oscillator frequency at 3.9 kHz to enable phase-sensitive detection of the CPT resonance (Fig. 5(a)). The resulting signal from the lock-in amplifier is shown in Fig. 6(a), where the magnetic flux density has been changed in 2.53 nT steps. The currents passing through the ITO heaters and a thermoelectric element (used to temperature stabilize the base plate on which the magnetic sensor sits) create a significant field gradient across the cell. This drastically broadens the  $|1, -1\rangle - |2, -1\rangle$  resonance peak width to 520 kHz, compared to 11.5 kHz for the magnetically insensitive  $|1, 0\rangle - |2, 0\rangle$  resonance. To eliminate the effects of the gradients, we chop the currents through the ITO heaters. When the currents are off, we measure the magnetic flux density using a CPT resonance that is 13.2 kHz wide. The currents are chopped at 40 Hz with a duty cycle of 50 %, and a sample-and-hold circuit is placed after the photodiode amplifier that samples the signal with a measurement duty cycle of 39.5 %. The reduction in measurement time degrades the sensitivity by only a factor of 1.6.

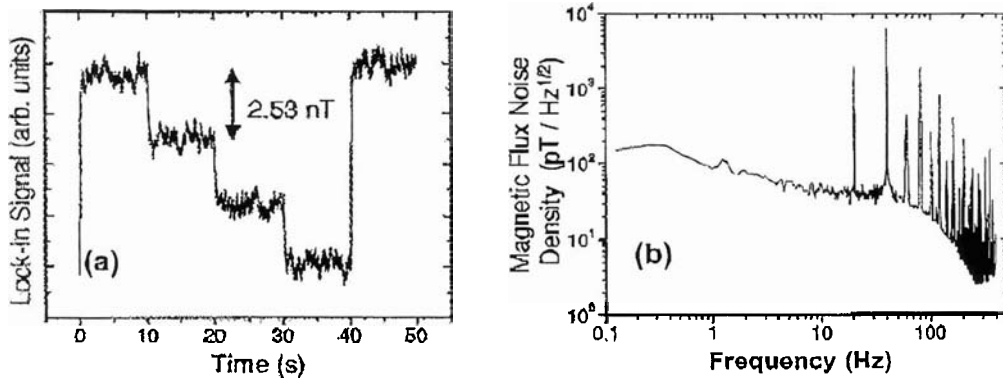


**Figure 6.** (a) The lock-in signal is plotted as a function of time as the magnetic flux is stepped in 10 s intervals. The lock-in time constant is 30 ms with a filter roll-off 24 dB/octave. The magnetic flux density during the measurement is nominally 73.9  $\mu\text{T}$ . (b) Power spectral density of the lock-in signal converted to units of magnetic flux density. The lock-in time constant is 1 ms with a filter roll-off 24 dB/octave (figure from ref. 12).

Figure 6(b) shows the noise spectrum of the CPT signal when the lock-in time constant is 1 ms. The demodulation frequency of the local oscillator is chosen to be 3.9 kHz, a half-integer harmonic of 40 Hz. Thus, the phase of the de-modulation frequency is reversed at the start of each measurement cycle giving rise to the 20 Hz peak in the lock-in noise spectrum. This eliminates a systematic error that would result from starting the measurement cycle at a constant demodulation phase by using an integer harmonic. To suppress the 20 Hz peak, a magnetic flux density measurement is performed with a time constant of 30 ms and a low-pass roll off of 24 dB/octave.

The present result clearly demonstrates that atom-optical magnetometers with millimeter dimensions can provide excellent performance. However, many aspects of the current magnetic sensor are not optimal, and in future devices we will both improve the sensitivity and reduce the power consumption.

Optimization of the VCSEL design and optics will improve the sensitivity by providing a more uniform light intensity distribution within the cell and reducing the VCSEL-related noise sources. The present sensor uses 195 mW of power, which can be reduced significantly by improving the microwave modulation efficiency of the VCSEL and redesigning the thermal isolation of the cell. Ultimately, the shot-noise-limited sensitivity of a CPT-based magnetic sensor will be  $1 \text{ pT Hz}^{-1/2}$ , while the power consumption can be reduced to less than 25 mW. We believe that an entire CPT magnetometer, including a 3.4 GHz oscillator and several control circuits, could be assembled that would dissipate  $< 50 \text{ mW}$  of power and have a volume of only  $1 \text{ cm}^3$ .

#### 4. Chip scale magnetometers based on atomic Zeeman transitions

The fundamental atom shot-noise-limited sensitivity for a  $1 \text{ mm}^3$  cell is,  $0.05 \text{ pT Hz}^{1/2}$  due to spin exchange collisions.<sup>18</sup> To approach this sensitivity it will be advantageous to implement atom optical schemes where the narrow Zeeman lines can be measured directly see Fig.3, negating the need for CPT

techniques. This energy is given by  $\Delta E = \frac{\mu_B g_s B_0}{(2I+1)} = 2\pi\hbar\gamma_s B_0$ , where  $\mu_B$  is the Bohr magneton,  $g_s \approx 2$  is the g-factor for an electron,  $\hbar$  is Planck's constant,  $I$  is the nuclear angular momentum and  $B_0$  is the magnitude of the applied field. An atom polarized perpendicular to the magnetic field will precess with angular frequency  $\omega_p = \Delta E / \hbar$ . For Rb, the proportionality constant between precession frequency  $f = 2\pi\omega_p$  and  $B_0$  is  $\gamma_s \approx 7.0 \text{ Hz/nT}$ . By measuring this precession frequency (or energy), it is therefore possible to determine the magnitude of the applied dc field,  $B$ .

In addition, to operate the hyperfine CPT magnetometer, the frequency of two different hyperfine transitions must be measured to subtract the  $\omega_{0,0}$  contribution to Eq. (1). Typically,  $\omega_{0,0}$  is measured once to calibrate the magnetometer for performing a series of magnetic field measurements using a magnetically sensitive transition. In general,  $\omega_{0,0}$  differs from the unperturbed atomic ground-state splitting mainly because of the buffer-gas shift, which is temperature dependent and requires periodic calibration.<sup>19</sup> This effect is not a problem in a Zeeman splitting measurement.

It is intriguing to consider some of the other types of atom-optical magnetometers that may benefit from MEMS miniaturization. We are currently developing a nonlinear magneto optical rotation (NMOR) system. NMOR magnetometers work on the principle that Zeeman excited atoms will rotate the polarization of a laser beam. In this method the one laser is used to both pump and probe the atoms. Figure 7(a) shows the components of a frequency modulated NMOR system. In principle, NMOR can be used to detect fields as low as  $1 \text{ fT Hz}^{-1/2}$  in a large cell. This is because the atomic polarization is maintained over thousands of collisions with the walls of the cell. Budker *et al.*<sup>6</sup> have recently observed ultra-narrow (1 Hz) zero-field resonances in NMOR with rubidium atoms with high-quality antirelaxation coatings in large cells. However, upon reduction of cell size to  $1 \text{ mm}^3$ , we estimate an ultimate field sensitivity of  $1 \text{ pT Hz}^{-1/2}$  (similar to the CPT magnetometer described above). The advantages of this method are several: the spin decoherence time for Zeeman states is typically longer than the hyperfine decoherence time,<sup>20</sup> the use of a balanced polarimeter to detect the optical rotation can eliminate much of the AM and FM-AM noise, and low frequency rf signals take less power to generate. However, several challenges must be addressed, including the development of an appropriate cell coating compatible with the vapor cell fabrication process, the development of wafer level batch fabricated polarizers and analyzers, and a small balanced detector.

Another approach that might work is to use the spin-exchange-relaxation-free (SERF) method developed by the Romalis *et al.*<sup>5</sup> At very low fields (< 100 nT) and at high alkali atom density spin exchange relaxation shot noise can be eliminated. The sensitivity is then determined by spin destruction collisions between colliding alkali atoms. SERF requires two orthogonal lasers, one for pumping and the other for probing the optical rotation of the vapor cell (Fig. 7(b)). The sensitivity of the technique has been experimentally demonstrated to be  $0.54 \text{ fT Hz}^{-1/2}$  with the potential for improvements to the  $10^{-3} \text{ fT}$  level in a large cell. We anticipate a shot noise limited sensitivity for a micro-fabricated SERF magnetometer with a  $1 \text{ mm}^3$  cell to be less than  $100 \text{ fT Hz}^{-1/2}$ . One problem with this approach is that the dynamic range is limited to 100 nT to take advantage of the spin-exchange suppression, however, it may be possible to use a set of feedback coils for operation outside of a magnetic shield.<sup>21</sup> Also, high laser power is required for polarizing the atoms and high cell temperatures are needed for the high vapor pressures needed for SERF. Finally, it may be difficult implement the transverse laser fields using MEMS fabrication methods.

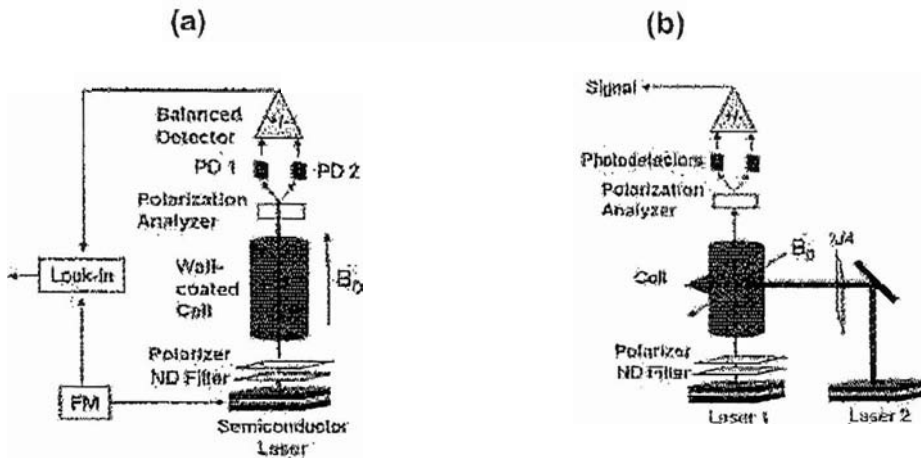
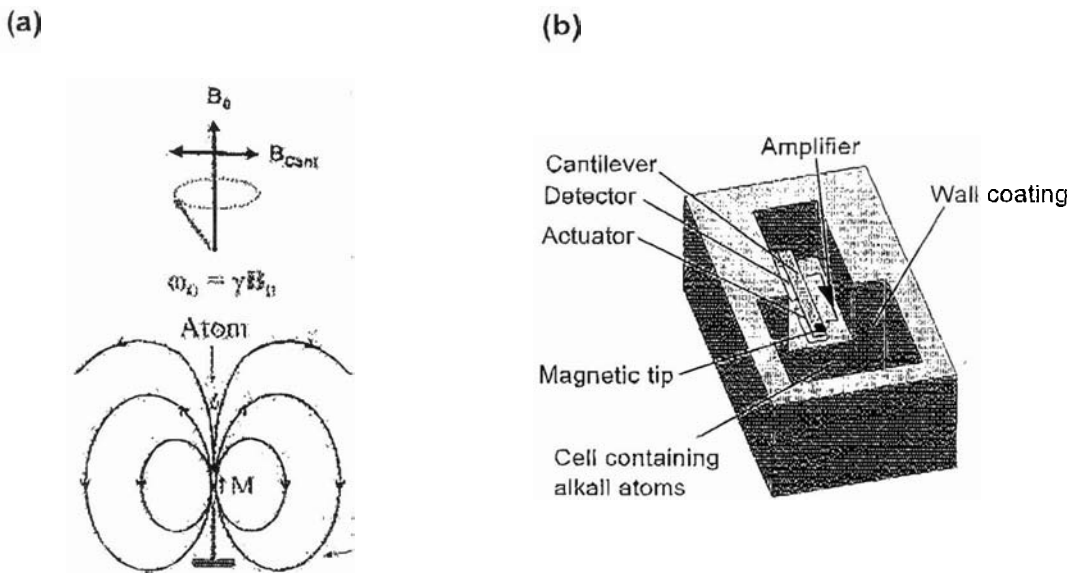


Figure 7. (a) Frequency modulated nonlinear magneto-optical rotation magnetometer (FM NMOR). (b) Spin-exchange-relaxation-free (SERF) magnetometer.

Finally, we are developing a novel device based on direct coupling between the “local oscillator” and the atoms. The idea is to let the energy of the oscillator bounce back and forth between the atoms and a magnetic mechanical resonator via direct magnetic coupling, eliminating the need for an electronic coupling mechanism. This concept is akin to a MASER where an RF resonator is replaced by a mechanical resonator.<sup>22</sup> If the energy of excitation of the atoms and the mechanical resonator are similar, a very compact, low power, atom/mechanical oscillator sensitive to magnetic field could be realized (tuning could be done by adjusting the mechanical resonator frequency to the Zeeman shift of the atoms, for example). Figure 8(a) shows a vibrating cantilever with a magnet on its tip coupling to an atom. As the cantilever moves the magnetic dipole is tilted about the azimuthal axis and it generates a transverse field at the Zeeman resonance frequency. A conceptual design for a micro-fabricated device is shown in Fig 8(b).



**Figure 8.** (a) Magnetic field lines from a small magnet mounted on a cantilever relative to atom located along the azimuthal axis showing how spin precession might be excited by the motion of magnetic resonator tip. (b) Components for a microfabricated direct-coupling atom/cantilever oscillator.

## Acknowledgments

This work was supported by the Microsystems Technology Office of the U.S. Defense Advanced Research Projects Agency (DARPA). This work is a contribution of NIST, an agency of the U.S. government, and is not subject to copyright.

## References

1. G. Boero, J. Frounchi, B. Furrer, P.-A. Besse, and R. S. Popovic, "Fully integrated probe for proton nuclear magnetic resonance magnetometry," *Rev. Sci. Instrum.* **72**, 2764, 2001.
2. G. Boero, M. Demierre, P.-A. Besse, R.S. Popovic, "Micro-Hall devices: Performance, technologies and applications," *Sensors and Actuators A* **106**, 314, 2003.
3. H. Lhermet, R. Cuchet, L. Vieux-Rochaz, and M.-H. Vaudaine, "Noise Measurements on NiFe/Ag Multilayered Structures," *IEEE Trans. Magn.* **36**, 3618, 2000.
4. P. Ripka, "Advances in fluxgate sensors," *Sensors and Actuators A* **106**, 8, 2003.
5. K. Kominis, T. W. Kornack, J. C. Allred, and M. V. Romalis. "A subfemtotesla multichannel atomic magnetometer," *Nature* **422**, 596 (2003).
6. D. Budker, D. F. Kimball, V. V. Yashchuk, and M. Zolotorev, "Nonlinear magneto-optical rotation with frequency-modulated light," *Phys. Rev. A* **65**, 055403, 2002.

7. H. Weinstock, (ed.), *SQUID Sensors: Fundamentals, Fabrication, and Applications*, (Kluwer Academic, Dordrecht, 1996).
8. J. Kitching, S. Knappe and L. Hollberg, "Miniature vapor-cell atomic frequency references," *Appl. Phys. Lett.* **81**, 553, 2002.
9. L.-A. Liew, S. Knappe, J. Moreland, H. Robinson, L. Hollberg, and J. Kitching, "Microfabricated Alkali Atom Vapor Cells," *Appl. Phys. Lett.* **84**, 2694, 2004.
10. S. Knappe, V. Shah, P. D. D. Schwindt, L. Hollberg, J. Kitching, L.-A. Liew, and J. Moreland, "A Microfabricated Atomic Clock," *Appl. Phys. Lett.* **85**, 1460, 2004.
11. S. Knappe, P. D. D. Schwindt, V. Shah, L. Hollberg, J. Kitching, L. Liew and J. Moreland, "A chip-scale atomic clock based on  $^{87}\text{Rb}$  with improved frequency stability," *Optics Express* **13**, 1249, 2005.
12. P. D. D. Schwindt, S. Knappe, V. Shah, L. Hollberg, J. Kitching, L.-A. Liew, and J. Moreland, "A Chip-Scale Atomic Magnetometer," *Appl. Phys. Lett.* **85**, 6409, 2004.
13. E. Arimondo, "Coherent population trapping in laser spectroscopy," *Progress in Optics*, **35**, 257, 1996.
14. A. Nagel, L. Graf, A. Naumov, E. Mariotti, V. Biancalana, D. Meschede and R. Wynands, "Experimental realization of coherent dark-state magnetometers," *Europhys. Lett.* **44**, 31, 1998.
15. M. Stähler, S. Knappe, C. Affolderbach, W. Kemp, R. Wynands, "Picotesla magnetometry with coherent dark states," *Europhys. Lett.* **53**, 323, 2001.
16. J. Kitching, S. Knappe, N. Vukicevic, L. Hollberg, R. Wynands, and W. Weidemann, "A microwave frequency reference based on VCSEL-driven dark line resonance in Cs vapor," *IEEE Trans. Instrum. Meas.* **49**, 1313, 2000.
17. R. Wynands, A. Nagel, S. Brandt, D. Meschede, and A. Weis, "Selection rules and line strengths of Zeeman-split dark resonances," R. Wynands, A. Nagel, S. Brandt, D. Meschede, and A. Weis, *Phys. Rev. A* **58**, 196, 1998.
18. J. C. Allred, R. N. Lyman, T. W. Kornack, and M. V. Romalis, "High-Sensitivity Atomic Magnetometer Unaffected by Spin-Exchange Relaxation," *Phys. Rev. Lett.* **89**, 130801 (2002).
19. J. Vanier and C. Audoin. *The Quantum Physics of Atomic Frequency Standards*. (Hilger, London 1989).
20. Y.-Y. Jau, A. B. Post, N. N. Kuzma, A. M. Braun, M. V. Romalis, and W. Happer, "Intense, Narrow Atomic-Clock Resonances," *Phys. Rev. Lett.* **92**, 110801, 2004.
21. S. J. Seltzer and M. V. Romalis. "Unshielded three-axis vector operation of a spin-exchange-relaxation-free atomic magnetometer." *Appl. Phys. Lett.* **85**, 4804, 2004.
22. I. Bargatin and M. L. Roukes, "Nanomechanical Analog of a Laser: Amplification of mechanical oscillations by stimulated Zeeman transitions," *Phys. Rev. Lett.* **91**, 138302, 2003.